



Optimizing proton exchange membrane fuel cell parameter identification using enhanced hummingbird algorithm[☆]

Manish Kumar Singla^{a,g}, Murodbek Safaraliev^b, Jyoti Gupta^c, Mohammad Aljaidi^d,
Ismoil Odinaev^{b,*}, Ramesh Kumar^{a,f}, Amir Abdel Menaem^{b,e}

^a Department of Interdisciplinary Courses in Engineering, Institute of Engineering & Technology, Chitkara University, Punjab, India

^b Department of Automated Electrical Systems, Ural Federal University, 620002, Yekaterinburg, Russia

^c School of Engineering and Technology, K. R. Mangalam University, 122003, Haryana, Gurgaon, India

^d Department of Computer Science, Zarqa University, 13110, Zarqa, Jordan

^e Electrical Engineering Department, Mansoura University, Mansoura 35516, Egypt

^f Jadara University Research Center, Jadara University, Jordan

^g Applied Science Research Center, Applied Science Private University, Amman, Jordan

ARTICLE INFO

Keywords:

Proton exchange membrane fuel cell
Optimization
Hydrogen
Enhanced algorithm
Sum of square error
Benchmark test function
Non-parametric test

ABSTRACT

Fuel cells (FCs) have attracted significant interest due to their versatile applications, but modeling their nonlinear behavior is challenging. This research proposes an Enhanced Artificial Hummingbird Algorithm (EAHA) to identify the seven unknown parameters of proton exchange membrane fuel cell (PEMFC) stacks using their experimental data. The goal is to accurately predict the current/voltage (I/V) curves by minimizing a cost function defined as the sum of squared differences between measured data points and model estimates. The EAHA combines several territorial foraging techniques with a linear regulation mechanism. Its performance is compared to the conventional Artificial Hummingbird Algorithm (AHA) using three common PEMFC modules. Additionally, a comparative analysis is performed against previously published methods and newly developed optimizers like Particle Swarm Optimizer (PSO), Grasshopper Optimization Algorithm (GOA), Atom Search Optimization (ASO), Grey Wolf Optimizer (GWO), and parental algorithm i.e., Artificial Hummingbird Algorithm (AHA). The findings showcase the proposed approach's efficacy relative to existing methods and state-of-the-art optimizers. The two models are taken for the checking of reliability and performance of the PEMFC. The results are also compared with the Non-Parametric tests and it is concluded that the proposed algorithm is far better than the rest of the compared algorithms in both the models.

1. Introduction

Proton exchange membrane fuel cells (PEMFCs) have emerged as a promising alternative energy conversion technology due to their high efficiency, low emissions, and diverse potential applications from transportation to stationary power generation [1,2]. However, accurately modeling the behavior of PEMFCs is a significant challenge because of their complex and nonlinear characteristics. Precisely estimating the model parameters is crucial for developing and optimizing PEMFC systems to enable efficient and reliable operation [3,4].

To enhance the longevity and robustness of PEMFCs, scientists and

researchers are actively pursuing various strategies [5]. These approaches involve utilizing advanced modeling and simulation techniques that play a key role in understanding the intricate processes occurring within PEMFCs [6,7]. These techniques harness the power of computational modeling and precise simulation tools to gain insights into the complex phenomena happening inside the fuel cell system. By employing mathematical models, researchers can optimize operational conditions, predict PEMFC lifespan, and investigate the factors influencing performance and degradation. This approach facilitates a thorough exploration of various operational and design parameters, leading to improvements in PEMFC durability and overall performance [8]. One

[☆] This paper is the English version of the paper reviewed and published in Russian in “International Scientific Journal for Alternative Energy and Ecology “. ISJAEE, 423, # 06 (2024).

* Corresponding author.

E-mail address: ismoil.odinaev@urfu.ru (I. Odinaev).

<https://doi.org/10.1016/j.ijhydene.2024.09.211>

Received 3 May 2024; Accepted 15 September 2024

Available online 28 September 2024

0360-3199/© 2024 Hydrogen Energy Publications LLC. Published by Elsevier Ltd. All rights are reserved, including those for text and data mining, AI training, and similar technologies.

notable application highlighting the potential of these advanced modeling techniques is integrating PEMFCs as the primary power source within a combined cooling, heating, and power system while simultaneously incorporating a heat recovery system.

The key to generating accurate simulations of PEMFCs lies in the parameter identification procedure, which involves selecting crucial parameters that characterize the behavior and operation of the PEMFC device [9]. Mathematical frameworks are used to predict the operation of the fuel cell, with the governing parameters specified based on well-established physical and electrochemical principles. To adjust the unidentified model variables to match experimental data, several parameter estimation methods are employed [10]. These techniques aim to minimize the difference between observed data and model predictions by iteratively changing the values of the parameters. Numerical modeling begins by formulating equation-based descriptions of the physical and electrochemical processes occurring inside the PEMFC. Partial differential equations are commonly utilized within this framework to express the conservation laws governing electrochemical reactions, mass transfer, momentum, energy, charge transfer, and other transport phenomena [11,12].

In recent years, the field of model parameter estimation for PEMFCs has seen significant advancements driven by the need to overcome the limitations of traditional modeling approaches and improve prediction accuracy. Accurate PEMFC modeling allows for a better understanding of their behavior, optimization of operating conditions, and design of control strategies to enhance performance.

Over recent decades, the application of soft computing technologies has gained significant traction in emulating the behavior of proton exchange membrane fuel cell (PEMFC) units and enhancing their overall performance. These advanced frameworks encompass a variety of techniques, including fuzzy logic rules [13], support vector machines [14], artificial neural networks [15], and neuro-fuzzy procedures [16]. By leveraging the capabilities of these soft computing methodologies, researchers have been able to capture and mimic the complex behavior of PEMFCs, paving the way for improved operational strategies and performance optimization.

Moreover, in recent years, PEMFC optimization has seen a surge in the development and implementation of heuristic-based optimizers. These optimizers are designed to determine the optimal values for the unknown parameters within PEMFC systems, ultimately enhancing their efficiency and performance [17]. In this rapidly evolving landscape, numerous optimization procedures have emerged, each offering unique advantages and capabilities. Notable examples of these optimization techniques include the Whale Optimizer (WO) [18], Hybrid Jellyfish Search Optimizer and Particle Swarm Optimization (HJSOPSO) [19], Modified Manta Ray Foraging Algorithm (MMRFA) [20], Improved Artificial Ecosystem Optimizer (IAEO) [21], Slime Mold Optimizer (SMO) [22], and Flower Pollination Optimizer (FPO) [23]. By leveraging nature-inspired concepts and computational intelligence, these algorithms efficiently explore the parameter space of PEMFCs, enabling the identification of optimal operating conditions and design configurations.

Beyond established methods, researchers actively investigate new optimization techniques to improve PEMFC performance and reliability. This includes a surge of novel algorithms like the Hybrid Marine Predator and Political Optimizer (HMPPPO) [24], Cooperative Barebone Particle Swarm Optimization (CBPSO) [25], and the Improved Chaotic Grey Wolf Optimization (ICGWO) [26]. Additionally, researchers explore algorithms like Elman Neural Networks (ENN) [27], and the Shuffled Multi-Simplexes Search (SMSS) [28]. Each approach brings unique strengths, enriching the toolbox for PEMFC optimization.

This research introduces an Enhanced Artificial Hummingbird Algorithm (EAHA) to address these challenges. This method effectively extracts PEMFC parameters using a memory-saving strategy inspired by hummingbirds [29]. EAHA tackles the optimization problem of finding the seven unknown parameters in a PEMFC stack using real-world data.

It combines several search strategies inspired by how hummingbirds explore their territory [30,31]. These strategies allow the algorithm to explore different areas of the solution space thoroughly, balancing both broad exploration and targeted searching [32]. Additionally, a special mechanism is included to improve the algorithm's ability to find both broad and specific solutions [33]. This combined approach enhances the overall performance of EAHA. The key contributions of this work are:

- Improving the Artificial Hummingbird Algorithm (EAHA) to make it better at finding unknown settings (parameters) within PEMFC fuel cell stacks used in real-life situations.
- Validating the effectiveness of the EAHA on real-world PEMFC units by applying it to two specific models: Ballard Mark V and AVISTA SR-12.
- To demonstrate the superiority of the EAHA, it will be compared to established methods like Particle Swarm Optimizer (PSO), Grasshopper Optimization Algorithm (GOA), Atom Search Optimization (ASO), Grey Wolf Optimizer (GWO), and parental algorithm i.e., Artificial Hummingbird Algorithm (AHA).
- Ten Benchmark test function is also tested to verify the algorithm.

NOMENCLATURE

Nomenclature	
FCs	Fuel Cells
EAHA	Enhanced Artificial Hummingbird Algorithm
PEMFC	Polymer Electrolyte Fuel Cell/Proton Exchange Membrane Fuel Cell
AHA	Artificial Hummingbird Algorithm
PSO	Particle Swarm Optimizer
GOA	Grasshopper Optimization Algorithm
ASO	Atom Search Optimization
GWO	Grey Wolf Optimizer
WO	Whale Optimizer
HJSOPSO	Hybrid Jellyfish Search Optimizer and Particle Swarm Optimizer
MMRFA	Modified Manta Ray Foraging Algorithm
IAEO	Improved Artificial Ecosystem Optimizer
SMO	Slime Mold Optimizer
FPO	Flower Pollination Optimizer
HMPPPO	Hybrid Marine Predator and Political Optimizer
CBPSO	Cooperative Barebone Particle Swarm Optimization
ICGWO	Improved Chaotic Grey Wolf Optimization
ENN	Elman Neural Network
SMSS	Shuffled Multi-Simplexes Search
SSE	Sum of Squared Error
VTA	Visiting Table
SD	Standard Deviation
STC	Standard Temperature Conditions
AE	Absolute Error
Symbol	
I/V	Current/Voltage
T_{FC}	Cell Temperature
P_{H_2}	Partial Pressures of H_2
P_{O_2}	Partial Pressures of O_2
I_{FC}	FC Current
R_m	Membrane Resistance
R_c	Contact Resistance
ρ_m	Membrane's Resistivity
l	Membrane Thickness
A_m	Active Area of The Cell
J	Real Current Density
λ	Membrane Water Content
β	Maximum Current Density
J_{max}	Constant Coefficient
N_{cells}	Series of Cells
V_{stack}	Stack Voltage
V_{actual}	Actual Experiment Voltage
V_i	Computed Model Voltage
N	Number of Data Points
R_1	Random Point
L_L and U_L	Boundaries of The Landscape
c	Territorial Parameter

(continued on next page)

(continued)

Nomenclature	
G_{worst}	Food Source with The Lowest Nectar Refill Rate
t	Current Iteration
t_M	Maximum Number of Iterations

2. PEMFCS' modelling and problem formulation

PEMFC modeling uses mathematical equations and computer simulations to understand the chemical and electrical processes within the fuel cell. The PEMFC schematic representation is shown in Fig. 1.

PEMFCs experience voltage drops due to several factors:

- Activation losses: When the fuel cell starts operating (low load), slow initial reactions cause a rapid voltage drop.
- Ohmic losses: As the current increases, resistance to the flow of protons and electrons leads to a gradual voltage decline.
- Concentration losses: High power demands (heavy load) cause water buildup, reducing reactant concentration and leading to a significant voltage drop.

These voltage drops, collectively contributing to the overall voltage loss in the fuel cell, significantly impact the performance and efficiency of the system. Therefore, it is crucial to understand and minimize these voltage losses to enhance the performance of PEMFCs. Scientists and engineers employ various techniques to achieve this goal, such as catalyst development, improvements in flow field designs, and enhancements in reactant gas management.

Accordingly, Equation (1) may be used to represent the PEMFC terminal voltage:

$$V_{FC} = E_{Nernest} - v_{act} - v_{ohm} - v_{conc} \quad (1)$$

For temperatures that operate below 100°C, the reversible open-circuit voltage is represented by $E_{Nernests}$ which may be computed from Equation (2).

$$E_{Nernest} = 1.229 - 8.5 \times 10^{-4} \times (T_{FC} - 298.15) + 4.3085 \times 10^{-5} \times T_{FC} \times \ln(P_{H_2} \sqrt{P_{O_2}}) \quad (2)$$

where T_{FC} is the cell temperature (K) and P_{H_2} and P_{O_2} denote the partial pressures of H_2 and O_2 , correspondingly.

According to Equation (3), the activation voltage loss (v_{act}) is

approximated.

$$v_{act} = - [\xi_1 + (\xi_2 \times T_{FC}) + (\xi_3 \times T_{FC} \times \ln(C_{O_2})) + (\xi_4 \times T_{FC} \times \ln(I_{fc}))] \quad (3)$$

Where the FC current is defined as I_{FC} , and make use of the coefficients ξ_1 to ξ_4 . C_{O_2} and C_{H_2} and indicate the oxygen concentration (mol/cm³), which has the following definitions as shown in Equation (4) and Equation (5):

$$C_{O_2} = \frac{P_{O_2}}{5.08 \times 10^6} \times \exp\left(\frac{498}{T_{FC}}\right) \quad (4)$$

$$C_{H_2} = \frac{P_{H_2}}{1.09 \times 10^6} \times \exp\left(\frac{-77}{T_{FC}}\right) \quad (5)$$

The v_{ohm} is defined as follows and is calculated using the FC's equivalent resistance as shown in Equation (6):

$$v_{ohm} = I_{FC} \times (R_m + R_c) \quad (6)$$

Where R_m and R_c stand for the membrane resistance and the contact resistance, accordingly. Equation (7) and Equation (8) can be used to determine the R_m .

$$R_m = \frac{\rho_m \times l}{M_A} \quad (7)$$

$$\rho_m = \frac{181.6 \times [1 + 0.03 \times J + 0.062 \times J^{2.5} \times (T_{FC}/303)^2]}{[\lambda - 0.634 - 3 \times J] \times \exp(4.18 \times (T_{FC} - 303)/T_{FC})} \quad (8)$$

Where ρ_m , l , A_m , J and λ indicate, accordingly, the membrane's resistivity ($\Omega \cdot \text{cm}$), membrane thickness (cm), active area of the cell (cm²), real current density (A/cm²), and membrane water content.

The formula Equation (9) can be utilized for estimating the v_{conc} .

$$v_{conc} = -\beta \times \ln(1 - J/J_{max}) \quad (9)$$

Where β indicates the maximum current density (A/cm²) and J_{max} signifies a constant coefficient.

The PEMFC stack is often made up of a series of cells (N_{cells}), and the stack voltage is determined (V_{stack}) as shown in Equation (10):

$$V_{stack} = N_{cells} \times V_{FC} = N_{cells} \times (E_{Nernest} - v_{act} - v_{ohm} - v_{conc}) \quad (10)$$

By using the previously described equation while assuming that all of

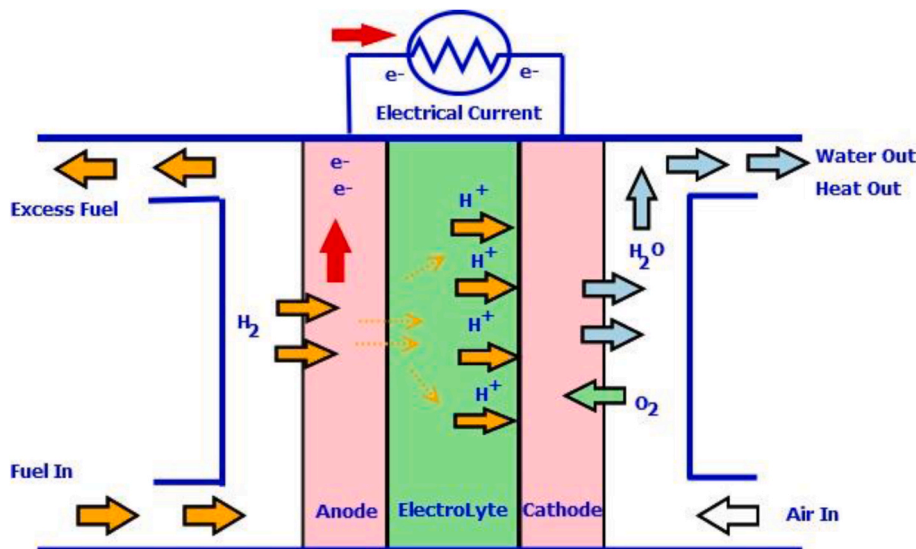


Fig. 1. Schematic representation of PEMFC.

the cells behave uniformly and that the resistors that link them are disregarded.

Seven unknown variables (ξ_1 to ξ_4 , λ , and β) need to be determined to fully define the mathematical model based on electrochemistry. An iterative process involving refinement, optimization, and validation is used to estimate these parameters in Mann’s model [34]. To achieve accurate and dependable parameter values that reflect real-world PEMFC behavior, a combination of experimental data, computer modeling, and optimization techniques is crucial. This applies not only to Mann’s model but also to any mathematical model. In essence, parameter optimization aims to find the values that minimize the gap between the model’s predictions and actual experimental results.

2.1. Problem formulation

This paper proposes a method to improve the accuracy of a PEMFC model by aligning its predicted output voltage with real-world measurements. The model uses mathematical formulas and known parameters to predict the voltage for any given current density. To achieve better alignment, a proposed algorithm is employed. The effectiveness of this approach is evaluated by comparing the predicted voltage with measured voltage data using the Sum of Squared Error (SSE) metric. Equation (11) details the objective function used in this evaluation.

$$SSE = \text{MIN} \left(F = \sum_{i=1}^N (V_{\text{actual}} - V_i)^2 \right) \quad (11)$$

Where, actual experiment voltage is denoted by V_{actual} , computed model voltage is denoted by V_i , and N is denoted as the number of data points.

3. Proposed algorithm

3.1. Developed EAHA

The AHA algorithm, inspired by how hummingbirds remember food sources [29], is a powerful optimization technique. This section introduces an improved version of AHA, called EAHA, which can find the unknown properties of a solar diode. Imagine a group of hummingbirds, each with its favorite feeding spot. Each hummingbird remembers the exact location and how quickly its nectar supply refills. They also recall how long it takes to fly back and forth. This unique ability allows them to efficiently find the best food sources. Similarly, EAHA works by simulating a swarm of “virtual hummingbirds.” These “hummingbirds” are randomly assigned to different potential solutions (like food sources). They then explore these solutions and remember how good they are (like how much nectar is available). Over time, the “hummingbirds” focus on the best solutions, just like real hummingbirds finding the tastiest nectar.

The mathematical details of this process are described in Equation (12), where a certain number of “hummingbirds” are randomly assigned to explore different possibilities.

$$G_h = R_1 \times U_L + (1 - R_1) \times L_L \quad h = 1, 2, \dots, g_m \quad (12)$$

Where R_1 is a random point within this “food landscape,” ranging from 0 to 1. The limits, L_L and U_L , mark the boundaries of this landscape. Each “food source,” denoted by G_h , represents a possible solution for the Solar PV model. We have several “hummingbirds” (g_m) searching for the best solution.

These “hummingbirds” are like real ones, remembering how long it takes to revisit a food source. To mimic this, author create a “visiting table” (VTA) that tracks how often each “hummingbird” visits each “food source.” This table helps them focus on promising solutions and avoid wasting time on unproductive ones as shown in Equation (13).

$$VTA_{hj} = \begin{cases} \text{null} & \text{if } h = j \\ 0 & \text{else} \end{cases} \quad (13)$$

$j = 1, 2, 3 \dots g_m, k = 1, 2, 3 \dots g_m$

Where null signifies that there is no value and $VTA_{k,j}$ shows how many times the hummingbird (h) skipped the source of nourishment (j).

The hummingbirds in the AHA algorithm searching for the best food sources. They do this using three different “flying styles”:

- **Straight Shot (Axial Flight):** Like a hummingbird zipping directly to a flower, the algorithm explores the search space in a straight line, focusing on a specific direction that seems promising. This helps them find good solutions quickly (Equation (14) shows how this works).
- **Sideways Hop (Diagonal Flight):** Like a hummingbird flitting between flowers, the algorithm explores areas near promising solutions but also ventures a bit further out. This helps it find even better solutions without getting stuck in one place (Equation (15) shows the details).
- **Random Wander (Omnidirectional Flight):** Like a hummingbird fluttering around, the algorithm explores the entire search space, even areas that don’t seem promising at first. This helps it discover new possibilities and avoid getting trapped in dead ends. (Equation (16) shows the math behind this). By using these three different flying styles, the AHA algorithm balances exploring new areas and focusing on good solutions it already found. This helps it find the best solution possible.

$$DF^{(h)} = \begin{cases} 1 & \text{if } h = \text{rand}_i(1, D_m) \\ 0 & \text{else} \end{cases} \quad (14)$$

$$DF^{(h)} = \begin{cases} 1 & \text{if } h = P(j), j \in [1, m], P = \text{randperm}(m), m \in [2, \lceil r_1 \times (D_m - 2) \rceil + 1] \\ 0 & \text{else} \end{cases} \quad (15)$$

$$DF^{(h)} = 1, h = 1, 2, \dots, D_m \quad (16)$$

The artificial hummingbird algorithm (AHA) mimics the three foraging strategies used by hummingbirds: directed, territorial, and migratory. In the directed and territorial strategies, one of the flying skills described in Equations (14)–(16) is randomly selected. When using the directed strategy, the hummingbird searches for a specific food source, eventually locating a potential nectar location. This potential food location is represented by r_1 , which is a randomized number between 0 and 1. D_m denotes the number of design variables, which are the seven unknown parameters being optimized. rand_i and $\text{rand}_{\text{perm}}$ are functions that randomly generate integers and integer permutations, respectively as shown in Equation (17).

$$G_{h,t}(t+1) = G_h(t) + a \times DF \times (G_h(t) - G_{h,t \text{ arg et}}(t)) \quad (17)$$

The current position of a food source (h) at time t is denoted by $G_h(t)$, while the desired or target position is $G_{h,t \text{ target}}(t)$. The movement towards the target location follows a Gaussian distribution represented by the variable a . So in the territorial strategy, the hummingbird explores the region adjacent to its territory seeking newer food locations based on the current and desired positions defined above.

The second foraging strategy employed by hummingbirds is territorial foraging. In this strategy, the hummingbird searches for fresher food sources near the boundaries of its small territory as shown in Equation (18):

$$G_{h,t}(t+1) = G_h(t) + c \times DF \times G_j(t) \quad (18)$$

Where in c represents a territorial parameter.

The update method of every nutritional source’s site (h) for the two strategies is shown in the following manner in Equation (19):

$$G_h(t+1) = \begin{cases} Gn_h(t+1) & \text{if } O(Gn_h(t+1)) < O(G_h(t)) \\ G_h(t) & \text{else} \end{cases} \quad (19)$$

$$j = 1, 2, 3, \dots, g_m$$

The third foraging strategy employed by hummingbirds is migratory foraging. This strategy is used when food sources are scarce in the hummingbird’s current area. In migratory foraging, if the hummingbird is positioned at the food source with the lowest nectar refill rate, represented by the fitness value $O(\cdot)$, it will abandon this source and migrate to a different randomly selected source in the broader search space. This migration occurs if the nectar refill amount, i.e. the fitness value, of the new source exceeds that of the currently available source. So when resources are scarce locally, the hummingbird migrates to a more distant, randomly found food location with a higher expected nectar availability as shown in Equation (20).

$$G_{\text{worst}} = r \times U_L + (1 - r) \times L_L \quad (20)$$

G_{worst} represents the food source with the lowest nectar refill rate among all the sources visited by the flock of hummingbirds. If a hummingbird moves beyond the search space limits, its position is reset to a random location within the bounds. This constraint handling allows the algorithm to fully explore the feasible region defined by the minimum and maximum values along each dimension. A boundary check procedure needs to be implemented to ensure the hummingbirds stay within the search space. If any dimension parameter is violated, meaning a hummingbird flies outside the bounds, the position is returned back inside the borders in the following Equation (21):

$$G_h^{(d)}(t+1) = \begin{cases} L_L^{(d)}, & \text{if } G_j^{(d)}(t+1) < L_L^{(d)} \\ U_L^{(d)}, & \text{if } G_j^{(d)}(t+1) > U_L^{(d)} \\ G_h^{(d)}(t+1), & \text{else} \end{cases} \quad (21)$$

$$h = 1, 2, 3, \dots, g_m, d = 1, 2, 3, \dots, D_m$$

An important aspect of the AHA is the visiting table, which keeps track of the food sources visited by each hummingbird. This table allows each hummingbird to identify its preferred food source that it revisits. The visiting table shown in Equation (11) is unique for each hummingbird and gets updated over time as new sources are explored. By retaining memory of the most productive food locations discovered, the visiting table enables more informed search by guiding the hummingbirds back to high quality nectar sites as shown in Equation 22–24.

$$VTA_{h,k} = VTA_{h,k} + 1, \text{ if } k \neq h \& k \neq t \text{ arg et}, k = 1, 2, 3, \dots, g_m \quad (22)$$

$$VTA_{h,t \text{ arg et}} = 0 \quad (23)$$

$$VTA_{h,k} = \max_{L \neq h \& L \in g_m} (VTA_{h,L}) + 1, \text{ if } k \neq h, k = 1, 2, 3, \dots, g_m \quad (24)$$

A longer unvisited period in the visiting table indicates a higher visiting frequency for that food source. This table records the length of time each source has gone unvisited by a particular hummingbird since its last visit. So the visiting table tracks when each hummingbird last visited every food source, enabling the hummingbirds to return frequently to the most productive nectar locations. The proposed enhancements in the EAHA seek to further improve the foraging strategies and overall performance. The enhanced artificial hummingbird algorithm (EAHA) includes modifications and additional components to improve on the original AHA. The guided foraging strategy is adapted in the following key ways as shown in Equation (25):

$$Gn_h(t+1) = G_{h,t \text{ arg et}}(t) - (DF \times a \times [G_h(t) - G_q(t)]) \quad (25)$$

where the locations of the current (h) and random (q) sources of nutrition (h) at time t are denoted by the variables $G_h(t)$ and $G_q(t)$, and q represents an arbitrary integer value that has the following definition as shown in Equation (26):

Table 1
Benchmark test function.

Name of Function	Function	Range	Dimension
$f_1 = \text{Sphere}$	$f_1(y) = \sum_{j=1}^m y_j^2$	[-100,100]	m = 40
$f_2 = \text{Schwefel 2.22}$	$f_2(y) = \sum_{j=1}^m y_j + \prod_{j=1}^m y_j $	[-10,10]	m = 40
$f_3 = \text{Schwefel 1.2}$	$f_3(y) = \sum_{j=1}^m (\sum_{i=1}^j y_i)^2$	[-100,100]	m = 40
$f_4 = \text{Schwefel 2.21}$	$f_4(y) = \max_j \{ y_j , 1 \leq j \leq m\}$	[-100,100]	m = 40
$f_5 = \text{Rosenbrock}$	$f_5(y) = \sum_{j=1}^m 100(y_j + 1 - y_j^2)^2 + (y_j - 1)^2$	[-30,30]	m = 40
$f_6 = \text{Step}$	$f_6(y) = \sum_{j=1}^m ([y_j + 0.5])^2$	[-100,100]	m = 40
$f_7 = \text{Quartic}$	$f_7(y) = \sum_{j=1}^m j y_j^4 + \text{randm}[0, 1]$	[-128,128]	m = 40
$f_8 = \text{Schwefel}$	$f_8(y) = \sum_{j=1}^m -y_j \text{Sin}(\sqrt{ y_j })$	[-500,500]	m = 40
$f_9 = \text{Rastrigin}$	$f_9(y) = \sum_{j=1}^m [y_j^2 - 10 \text{Cos}(2\pi y_j) + 10]$	[-5.12,5.12]	m = 40
$f_{10} = \text{Ackley}$	$f_{10}(y) = -20 \exp(-0.2(\frac{1}{m} \sum_{j=1}^m y_j^2)^{0.5}) - \exp(\frac{1}{m} \sum_{j=1}^m \text{Cos}(2\pi y_j)) + 20 + e$	[-32,32]	m = 40

$$q = \text{rand}_i(1, g_m), q \neq h \quad (26)$$

The enhancement to the directed foraging strategy guides the search trajectories away from just the current best solution and towards additional nearby high quality options. Previously, only the precise position of the current best was employed. Expanding the neighborhood exploration around other competitive solutions, rather than solely exploiting the current best location, enables more effective and justified exploitative actions.

The territory forage approach also incorporates the subsequent types of territorial feeding as shown in Equation (27):

$$Gn_h(t+1) = \begin{cases} G_h(t) \times (1 + b \times DF) & \text{if } \text{rand} < 1/3 \\ G_h(t) \times (b \times [1 - G_q(t)] \times DF + 1) & \text{if } 1/3 < \text{rand} < 2/3 \\ G_q(t) \times (b \times [1 - G_q(t)] \times DF + 1) & \text{else} \end{cases} \quad (27)$$

The enhancement to the territorial foraging strategy incorporates information sharing between neighboring hummingbirds, rather than having each bird rely solely on its own experience. By exchanging details about food source locations, hummingbirds can better identify and seek out potentially undiscovered sources within their nearby territory. This facilitates more exploratory behavior within their vicinities.

Additionally, a linear tuning mechanism is employed to produce an adjustable parameter (θ) as shown in equation (28):

$$\theta = \frac{t}{t_M} \quad (28)$$

Where t denotes the current iteration number and t_M is the maximum number of iterations. The parameter θ increases linearly over time, modulating the foraging and exploitation tendencies of the enhanced algorithm. This gradual linear growth of θ serves to control and balance the exploration and exploitation behaviors.

Initially, with the territorial strategy in Equation (27), the hummingbirds display 100% exploratory searching. But as the algorithm

Table 2 (a)
Statistical results of benchmark test functions.

Algorithms		f ₁	f ₂	f ₃	f ₄	f ₅
PSO	MEAN	6.76E+00	1.84E+01	2.01E+04	2.98E+01	9.46E+03
	SD	4.67E+00	3.23E+01	8.79E+03	2.60E+01	1.21E+04
GOA	MEAN	2.24E-01	1.21E-12	2.94E+03	1.54E+01	2.59E+03
	SD	7.57E-02	2.74E-13	1.56E+03	5.08E+00	2.85E+03
ASO	MEAN	3.97E-25	2.76E-30	3.44E-18	7.79E-01	2.60E+00
	SD	2.93E-25	5.28E-30	4.62E-18	3.23E-01	3.28E-01
GWO	MEAN	1.84E-65	1.64E-38	1.56E-23	2.01E-16	2.62E+01
	SD	2.69E-65	1.51E-38	1.23E-23	1.23E-16	7.28E-01
AHA	MEAN	7.71E-193	1.45E-99	7.18E-146	1.41E-92	2.68E+01
	SD	0	3.5E-99	2.3E-145	4.04E-92	1.66E-01
Proposed Algorithm	MEAN	0	2.57E-109	0	3.74E-116	1.34E-03
	SD	0	4.5E-109	0	5.9E-132	2.17E-03

Table 2 (b)
Statistical results of benchmark test functions.

Algorithms		f ₆	f ₇	f ₈	f ₉	f ₁₀
PSO	MEAN	3.07E+01	6.29E-02	-6.13E+02	1.15E+02	1.17E+01
	SD	1.30E+01	2.95E-02	9.48E+01	3.39E+01	1.00E+01
GOA	MEAN	2.75E-01	4.69E-02	-5.95E+03	1.08E+02	1.05E+00
	SD	2.49E-01	2.44E-02	7.90E+02	1.71E+01	7.05E-01
ASO	MEAN	1.13E-02	4.93E-03	-1.10E+04	7.73E+01	7.61E-13
	SD	1.00E-02	2.18E-03	8.07E+02	2.22E+01	3.32E-13
GWO	MEAN	1.01E-03	5.20E-04	-2.55E+03	3.85E+01	1.51E-14
	SD	3.32E-04	4.62E-04	2.38E+02	7.52E+00	3.33E-30
AHA	MEAN	4.36E-05	4.70E-04	-7.43E+03	5.07E+00	8.88E-15
	SD	7.32E-05	2.08E-04	6.62E+02	1.44E+00	0
Proposed Algorithm	MEAN	3.06E-25	5.66E-05	-1.26E+04	0	8.88E-17
	SD	1.44E-25	2.89E-05	6.07E-02	0	0

iterates, the exploitative activity guided by the directed strategy in Equation (25) rises steadily, while the exploration guided by the territorial strategy in Equation (27) diminishes proportionately to the evolving scale of θ .

4. Results and discussion

In this two section are there, in the first section benchmark test functions are tested and in the second section an engineering problem is tested. Both the sections are explained below:

4.1. Benchmark test functions

To assess the effectiveness of the new algorithm, ten benchmark functions were chosen for testing. Table 1 summarizes these functions. The first seven (f1-f7) have a single minimum value (uni-modal), while the last three (f8-f10) have multiple minimum values (multi-modal). All functions have 40 variables. The performance of the new enhanced algorithm is compared against established optimization algorithms: Particle Swarm Optimization (PSO), Grasshopper Optimization Algorithm (GOA), Atom Search Optimization (ASO), Artificial Hummingbird Algorithm (AHA), and Grey Wolf Optimizer (GWO). All algorithms were evaluated for the same number of function calls (Max NFEs = 1000) across the ten benchmark functions. Each algorithm was run independently 40 times and all codes were implemented in MATLAB 2018b.

Tables 2(a) and Table 2(b) displays the average (mean) and SD (standard deviation) of the results obtained by each algorithm on the ten benchmark functions. Based on Table 2, the proposed algorithm appears to outperform the compared algorithms. This is evident from proposed algorithm achieving consistently better mean and standard deviation values across all ten test functions. Benchmark functions provide a standardized way to assess the effectiveness of new algorithms. In this case, the results suggest that proposed algorithm demonstrates better convergence speed, robustness, precision, and overall performance compared to the established algorithms.

Table 3
Parameter search range.

Parameter	Lower bound	Upper bound
ξ_1	-1.1997	-0.08532
$\xi_2 * 10^{-3}$	0.8	6.00
$\xi_3 * 10^{-5}$	3.60	9.80
$\xi_4 * 10^{-4}$	-2.60	-0.954
λ	10.00	24.00
$R_c * 10^{-4}$	1.00	8.00
b	0.0136	0.5

Table 4
Data sheet for the parameter estimation.

Model	Ballard Mark V	Avista SR-12
n	35	48
A [cm²]	50.6	62.5
l [um]	178	25
J_{max} [A/cm²]	1.5	0.672
P_{H2} [bar]	1	1.47628
P_{O2} [bar]	1	0.2095
Power [W]	1000	500
T [K]	343.15	323.15

4.2. Engineering problem

4.2.1. Parameter extraction of PEMFC

This section further investigates proposed algorithm performance by applying it to extract parameters for two different PEMFC models. Table 3 details the allowable range for each parameter in both models. Table 4 presents the data used for parameter estimation. To assess proposed algorithm effectiveness, it is compared against established optimization algorithms: Particle Swarm Optimization (PSO), Grasshopper Optimization Algorithm (GOA), Atom Search Optimization (ASO), Artificial Hummingbird Algorithm (AHA), and Grey Wolf

Table 5
Parameter estimation of PEMFC model of Ballard mark V.

Parameter/Algorithms	ξ_1	ξ_2	ξ_3	ξ_4	λ	R_c	b	SSE
PSO	-1.177	0.001	0.00003	-0.00026	11.038	0.0001	0.0136	1.20E-02
GOA	-1.173	0.001	3.63E-05	-0.00023	10	0.0001	0.0144	1.02E-03
ASO	-1.199	0.002	0.00003	-0.00026	10	0.0001	0.0247	1.13E-04
GWO	-1.199	0.002	4.36E-05	-0.00026	12.983	0.0002	0.1787	1.06E-04
AHA	-1.179	0.001	3.85E-05	-0.00026	10.013	0.0001	0.0241	1.18E-08
Proposed Algorithm	-1.168	0.001	4.51E-05	-0.00025	10.004	0.0002	0.0204	1.93E-10

Table 6
Parameter estimation of PEMFC model of Avista SR-12.

Parameter/Algorithms	ξ_1	ξ_2	ξ_3	ξ_4	λ	R_c	b	SSE
PSO	-0.907	0.001	0.00009	-0.0002	10	0.0001	0.0136	3.76E+00
GOA	-1.191	0.001	6.84E-05	-0.0002	13.720	0.0001	0.0655	1.00E+00
ASO	-0.997	0.001	9.06E-05	-0.0002	11.326	0.0002	0.1505	8.82E-01
GWO	-1.030	0.001	9.58E-05	-0.0002	10.180	0.0001	0.0138	8.21E-05
AHA	-0.922	0.001	9.53E-05	-0.0002	10.232	0.0001	0.0143	7.94E-12
Proposed Algorithm	-1.127	0.001	6.28E-05	-0.0002	13.757	0.0003	0.1647	3.89E-15

Table 7
Statistical results of PEMFC Model of Ballard Mark V.

Algorithms	Minimum	Average	Maximum	Mean	S.D	Error
PSO	1.20E-02	2.30E-02	5.89E-02	2.30E-02	1.38E-02	SSE
GOA	1.02E-03	1.37E-03	1.84E-03	1.37E-03	2.68E-04	
ASO	1.13E-04	1.54E-04	2.03E-04	1.54E-04	3.39E-05	
GWO	1.06E-04	1.73E-04	2.95E-04	1.73E-04	6.78E-05	
AHA	1.18E-08	3.09E-08	7.64E-08	3.09E-08	2.21E-08	
Proposed Algorithm	1.93E-10	4.08E-10	9.44E-10	4.08E-10	2.58E-10	

Optimizer (GWO). Setting the same limit for function evaluations (Max NFEs = 1000) for all algorithms across both models. Using a population size of 50 for each algorithm. Running each algorithm independently 40 times and implementing all codes in MATLAB 2018b.

4.2.2. Analysis of solution accuracy

Tables 5 and 6 present the best-found parameters and their corresponding Sum of Squared Errors (SSE) for the Ballard Mark V and Avista SR-12 PEMFC models, respectively. These results were obtained under standard temperature conditions (STC). An analysis of Tables 5 and 6 reveals that the proposed algorithm consistently achieves the lowest SSE values compared to the other algorithms. This indicates that proposed algorithm finds parameter sets that better match the experimental data for both PEMFC models. Further confirmation of proposed algorithm effectiveness comes from the statistical results presented in Tables 7 and 8, also obtained under STC. These tables and Fig. 2 suggest that proposed algorithm generally performs better than the other algorithms across various statistical metrics.

Table 8
Statistical results of PEMFC Model of Avista SR-12.

Algorithms	Minimum	Average	Maximum	Mean	S.D	Error
PSO	3.76E+00	5.97E+00	7.54E+00	5.97E+00	1.53E+00	SSE
GOA	1.00E+00	1.17E+00	1.42E+00	1.17E+00	1.52E-01	
ASO	8.82E-01	9.33E-01	9.95E-01	9.33E-01	3.88E-02	
GWO	8.21E-05	8.84E-05	9.85E-05	8.84E-05	6.37E-06	
AHA	7.94E-12	7.99E-12	8.03E-12	7.99E-12	4.29E-14	
Proposed Algorithm	3.89E-15	3.97E-15	4.04E-15	3.97E-15	4.85E-17	

SUM OF SQUARE ERROR

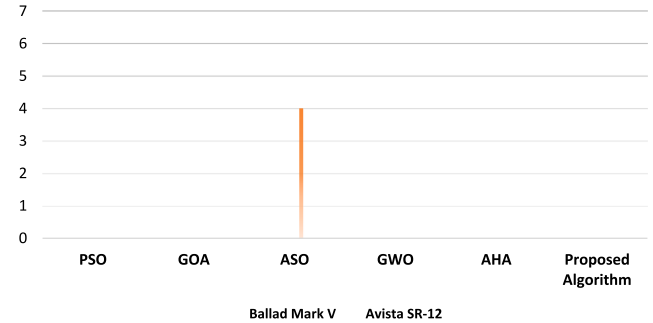


Fig. 2. SSE of both models.

COMPUTATIONAL TIME (SECS)

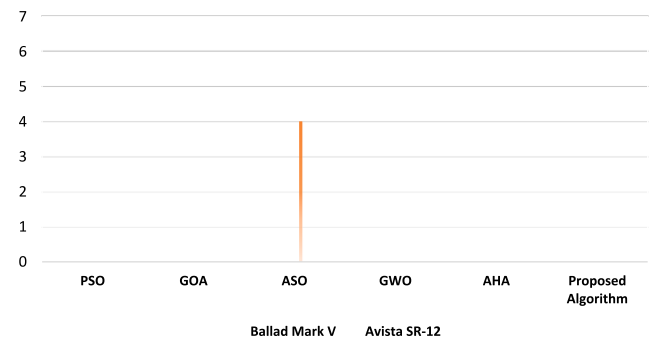


Fig. 3. Computational time of both models.

Table 9
Computational time (Sec) of both models.

Algorithms	Ballard Mark V	Avista SR-12	Statistical Analysis
PSO	3.112	3.452	Computational Time (Sec)
GOA	3.002	3.068	
ASO	2.854	2.984	
GWO	2.154	2.225	
AHA	1.547	1.698	
Proposed Algorithm	1.021	1.256	

4.2.3. Convergence analysis

Researchers compared the effectiveness of different optimization algorithms for proposed algorithm computations. From Table 9 and Fig. 3, it is clear that the proposed algorithm is far better than the parental algorithm as well as compared algorithms. The results demonstrate that the proposed algorithm converges significantly faster than the other compared algorithms.

Extracting the PEMFC model parameters using proposed algorithm allows for straightforward determination of the output voltage and power at various current levels. This accuracy is further supported by the data presented. Tables 10 and 11 show the measured output voltage, power, and absolute error (AE) for both models. Additionally, Figs. 4-7 illustrate the Voltage-Current (V-I) and Power-Current (P-I) curves. An analysis of these tables and figures suggests that proposed algorithm achieves superior performance and accuracy compared to the other tested algorithms for both PEMFC models.

Table 10
Calculated values of voltage, power and absolute error of model Ballard mark V.

Current Measured (A)	Voltage Measured (V)	Voltage Calculated (V)	Absolute Error (Voltage)	Power Measured (W)	Power Calculated (W)	Absolute Error (Power)
5.4	0.92	0.9204	4.00E-04	4.97	4.9689	1.10E-03
10.8	0.88	0.8798	2.00E-04	9.50	9.4999	1.00E-04
16.2	0.85	0.8498	2.00E-04	13.77	13.714	5.60E-02
21.6	0.82	0.8201	1.00E-04	17.71	17.7125	2.50E-03
27.0	0.79	0.7894	6.00E-04	21.96	21.9585	1.50E-03
32.4	0.77	0.7687	1.30E-03	24.95	24.94	1.00E-02
37.8	0.74	0.7401	1.00E-04	27.97	28.001	3.10E-02
43.2	0.72	0.7190	1.00E-03	31.10	31.09	1.00E-02
48.6	0.69	0.6894	6.00E-04	33.53	33.5247	5.30E-03
54.0	0.66	0.6604	4.00E-04	35.64	35.6154	2.46E-02
59.4	0.62	0.6198	2.00E-04	36.83	36.8245	5.50E-03
64.8	0.60	0.6200	2.00E-02	38.88	38.8798	2.00E-04
70.2	0.55	0.5501	1.00E-04	38.61	38.6054	4.60E-03
Sum of AE			2.52E-02			1.52E-01

Table 11
Calculated values of voltage, power and absolute error of model Avista SR-12.

Current Measured (A)	Voltage Measured (V)	Voltage Calculated (V)	Absolute Error (Voltage)	Power Measured (W)	Power Calculated (W)	Absolute Error (Power)
1.004	43.17	43.1698	2.00E-04	43.36	43.3458	1.42E-02
3.166	41.14	41.1354	4.60E-03	130.25	129.9987	2.51E-01
5.019	40.09	39.9989	9.11E-02	201.21	201.2054	4.60E-03
7.027	39.04	38.9939	4.61E-02	274.33	273.9878	3.42E-01
8.958	37.99	37.9784	1.16E-02	340.31	339.9897	3.20E-01
10.97	37.08	37.0412	3.88E-02	406.77	406.7548	1.52E-02
13.05	36.03	36.0254	4.60E-03	470.19	469.8979	2.92E-01
15.06	35.19	35.1547	3.53E-02	529.96	529.9458	1.42E-02
17.07	34.07	34.0574	1.26E-02	581.57	581.5548	1.52E-02
19.07	33.02	33.011	9.00E-03	629.69	629.6898	2.00E-04
21.08	32.04	31.9899	5.01E-02	675.40	675.3596	4.04E-02
23.01	31.20	31.1254	7.46E-02	717.91	717.9087	1.30E-03
24.94	29.80	29.7894	1.06E-02	743.21	743.1987	1.13E-02
26.87	28.96	28.9489	1.11E-02	778.16	778.1452	1.48E-02
28.96	28.12	28.1165	3.50E-03	814.36	814.3259	3.41E-02
30.81	26.3	26.2914	8.60E-03	810.30	809.9856	3.14E-01
32.97	24.06	24.0589	1.10E-03	793.26	793.2458	1.42E-02
34.90	21.40	21.3958	4.20E-03	746.86	746.8549	5.10E-03
Sum of AE			4.18E-01			1.71

4.2.4. Statistics analysis and robustness

The paragraph evaluates the performance of the proposed algorithm against other optimization algorithms, such as Particle Swarm Optimization (PSO), Grasshopper Optimization Algorithm (GOA), Atom Search Optimization (ASO), Artificial Hummingbird Algorithm (AHA), and Grey Wolf Optimizer (GWO). The evaluation was conducted using two datasets, Ballard Mark V and Avista SR-12, for parameter estimation of Proton Exchange Membrane Fuel Cell (PEMFC) models. The Friedman ranking test results, presented in Fig. 8 and Tables 12 and 13, showed that the proposed algorithm outperformed the other algorithms in terms of accuracy and precision, securing the top rank for both datasets. The AHA and GWO algorithms ranked second and third, respectively. To further validate the proposed algorithm’s performance, the Wilcoxon’s rank sum non-parametric test and the Kruskal-Wallis non-parametric test were applied. The Wilcoxon’s rank sum test (Tables 14 and 15) confirmed the proposed algorithm’s superior performance over the other algorithms at a 95% significance level. The Kruskal-Wallis test (Tables 16 and 17) also supported the proposed algorithm’s superiority by comparing the statistical differences among the algorithms [35–37]. Overall, the results from the various non-parametric tests conclusively demonstrated that the proposed algorithm exhibited higher precision and accuracy in parameter estimation of PEMFC models compared to the other evaluated optimization algorithms.

5. Conclusion

This paper proposes a new algorithm, called EAHA, to tackle challenges in finding the best possible solutions (global optimization) for

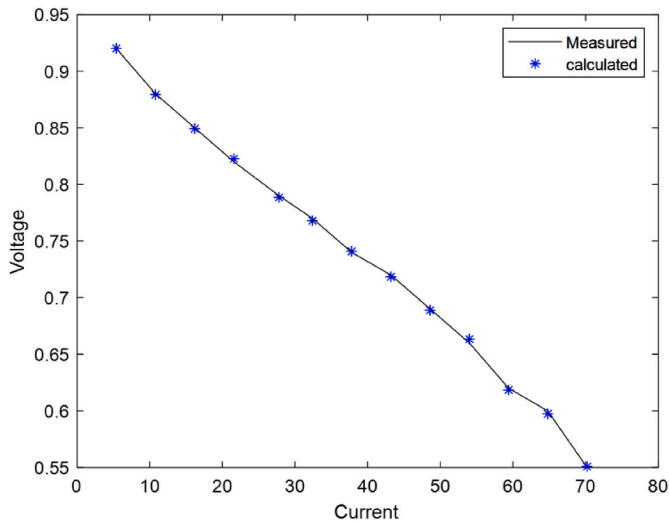


Fig. 4. Ballard mark V V-I characteristics curve.

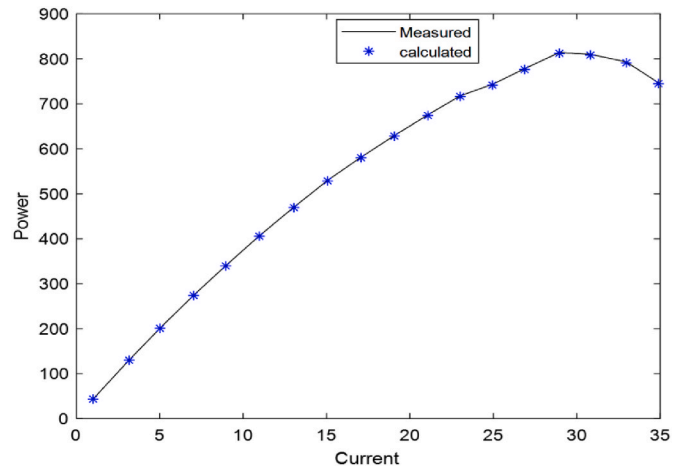


Fig. 7. Avista SR-12 P-I characteristics curve.

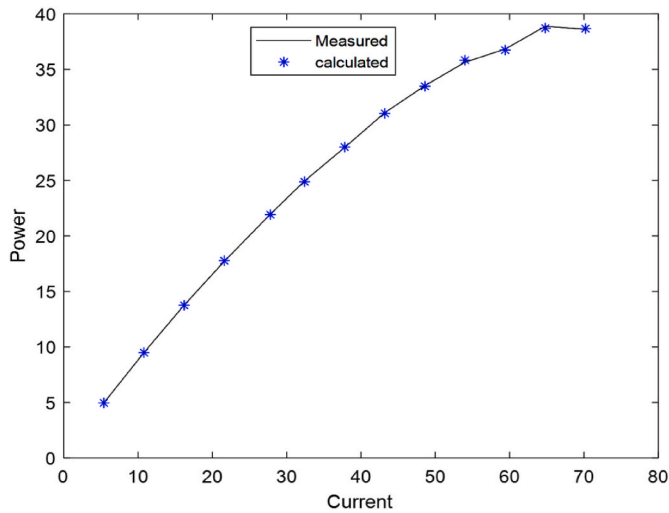


Fig. 5. Ballard mark V P-I characteristics curve.

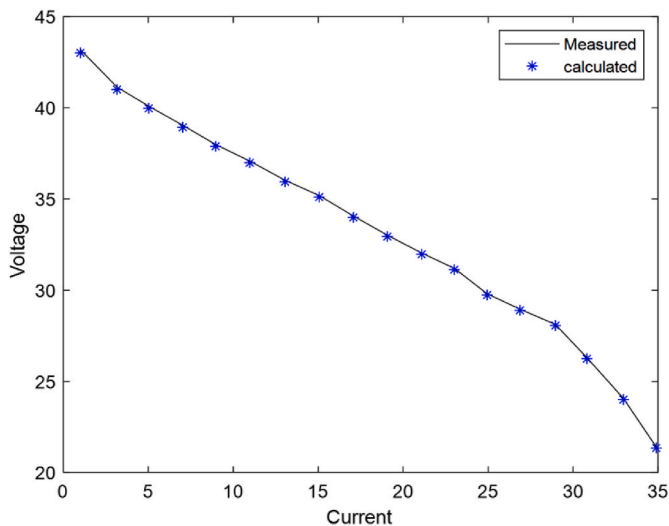


Fig. 6. Avista SR-12 V-I characteristics curve.

FRIEDMAN RANKING TEST

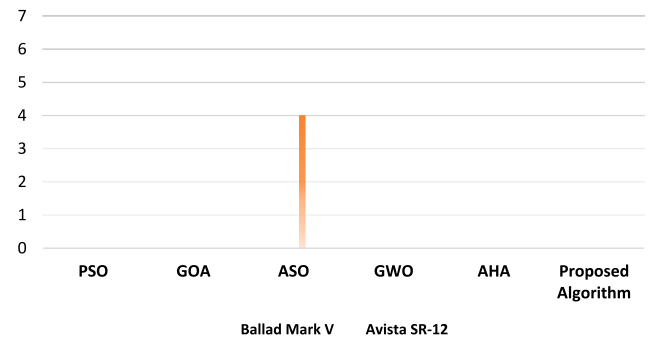


Fig. 8. Friedman Ranking Test of both models.

Table 12
Ballard mark V Friedman ranking test.

Algorithms	Friedman Ranking
PSO	6
GOA	5
ASO	4
GWO	3
AHA	2
Proposed Algorithm	1

Table 13
Avista SR-12 Friedman ranking test.

Algorithms	Friedman Ranking
PSO	6
GOA	5
ASO	4
GWO	3
AHA	2
Proposed Algorithm	1

different PEMFC models operating at various temperatures. The author applied EAHA to two specific PEMFC models: Ballard Mark V and Avista SR-12. To achieve this, author investigated the mathematical representation of the PEMFCs. The following section details the findings based on the obtained results:

Table 14

Ballard Mark V p values for Wilcoxon's Rank Sum.

Algorithms	PSO	GOA	ASO	GWO	AHA
Proposed Algorithm	3.9878E-13	3.9784E-13	3.9125E-13	3.9658E-13	3.9478E-13

Table 15

Avista SR-12 p values for Wilcoxon's Rank Sum.

Algorithms	PSO	GOA	ASO	GWO	AHA
Proposed Algorithm	3.8754E-11	3.8215E-11	3.8654E-11	3.8745E-11	3.8321E-11

Table 16

Ballard mark V Anova Kruskal-Wallis test.

Source	SS	df	MS	Chi-sq	Prob > Chi-sq
Columns	441762.1	4	90478.3	148.45	2.50254E-28
Error	32345.3	178	157.2	–	–
Total	474107.4	182	–	–	–

Table 17

Avista SR-12 Anova Kruskal-Wallis test.

Source	SS	Df	MS	Chi-sq	Prob > Chi-sq
Columns	448745.6	4	93587.3	178.03	7.54360E-38
Error	34657.7	178	254.3	–	–
Total	483403.3	182	–	–	–

- To validate the effectiveness of the newly developed Enhanced Artificial Hummingbird Algorithm (EAHA) for PEMFC model parameter extraction, author first tested it on ten benchmark functions. The results demonstrated superior performance by EAHA in terms of both solution accuracy and convergence speed for these global optimization problems.
- Furthermore, author applied EAHA to extract parameters for two PEMFC models (Ballard Mark V and Avista SR-12) operating at various temperatures. The resulting I–V and P–I characteristic curves were analyzed using statistical tests (Friedman ranking, Wilcoxon rank-sum, Kruskal-Wallis). These tests confirmed that EAHA achieved equivalent efficiency on both models compared to other algorithms. Overall, the statistical findings indicate that EAHA offers improved effectiveness for parameter extraction in PEMFC models.

5.1. Future scope

This study's findings suggest that the proposed algorithm has promising potential for estimating proton exchange membrane fuel cell parameters effectively. Notably, its applicability extends beyond this specific task. The algorithm's versatility allows its application to various other energy optimization challenges, making it a valuable tool for tackling diverse energy-related issues. Furthermore, its potential application in power systems could address crucial aspects like optimal distributed generation configuration, load dispatch, and energy scheduling problems. Optimizing these areas can potentially lead to improved system efficiency and successful outcomes.

References

- [1] Sultan HM, Menesy AS, Hassan MS, Jurado F, Kamel S. Standard and Quasi Oppositional bonobo optimizers for parameter extraction of PEM fuel cell stacks. *Fuel* 2023;340:127586.
- [2] Rezk H, Olabi AG, Abdelkareem MA, Sayed ET. Boosting the power density of two-chamber microbial fuel cell: modeling and optimization. *Int J Energy Res* 2022;46(15):20975–84.
- [3] Abd Elaziz M, Abualigah L, Issa M, Abd El-Latif AA. Optimal parameters extracting of fuel cell based on Gorilla Troops Optimizer. *Fuel* 2023;332:126162.
- [4] Samara G, Aljaidi M. Aware-routing protocol using best first search algorithm in wireless sensor. *Int Arab J Inf Technol* 2018;15(3A):592–8.
- [5] Özdemir MT. Optimal parameter estimation of polymer electrolyte membrane fuel cells model with chaos embedded particle swarm optimization. *Int J Hydrogen Energy* 2021;46(30):16465–80.
- [6] Shaheen A, El-Shehiemy R, El-Fergany A, Ginidi A. Fuel-cell parameter estimation based on improved gorilla troops technique. *Sci Rep* 2023;13(1):8685.
- [7] Yang S, Wang N. A novel P systems based optimization algorithm for parameter estimation of proton exchange membrane fuel cell model. *Int J Hydrogen Energy* 2012;37(10):8465–76.
- [8] Chang L, Li M, Qian L, de Oliveira GG. Developed multi-objective honey badger optimizer: application to optimize proton exchange membrane fuel cells-based combined cooling, heating, and power system. *Int J Hydrogen Energy* 2024;50:592–605.
- [9] Houssein EH, Hashim FA, Ferahtia S, Rezk H. An efficient modified artificial electric field algorithm for solving optimization problems and parameter estimation of fuel cell. *Int J Energy Res* 2021;45(14):20199–218.
- [10] Kandidayeni M, Macias A, Khalatbarisoltani A, Boulon L, Kelouwani S. Benchmark of proton exchange membrane fuel cell parameters extraction with metaheuristic optimization algorithms. *Energy* 2019;183:912–25.
- [11] Bai Q, Li H. The application of hybrid cuckoo search-grey wolf optimization algorithm in optimal parameters identification of solid oxide fuel cell. *Int J Hydrogen Energy* 2022;47(9):6200–16.
- [12] Aljaidi M, Aslam N, Samara G, Almatarneh S, Khaled AQ, Alqammaz A. EV charging station placement and sizing techniques: survey, challenges and directions for future work. In: *2022 international arab Conference on information technology (ACIT)*. IEEE; 2022, November. p. 1–6.
- [13] Aly M, Rezk H. An improved fuzzy logic control-based MPPT method to enhance the performance of PEM fuel cell system. *Neural Comput Appl* 2022;1–12.
- [14] Kheirandish A, Shafiqabady N, Dahari M, Kazemi MS, Isa D. Modeling of commercial proton exchange membrane fuel cell using support vector machine. *Int J Hydrogen Energy* 2016;41(26):11351–8.
- [15] Wilberforce T, Biswas M. A study into proton exchange membrane fuel cell power and voltage prediction using artificial neural network. *Energy Rep* 2022;8:12843–52.
- [16] Mostafaeipour A, Qolipour M, Goudarzi H, Jahangiri M, Golmohammadi AM, Rezaei M, Khalifeh Soltani SR. Implementation of adaptive neuro-fuzzy inference system (ANFIS) for performance prediction of fuel cell parameters. *Journal of Renewable Energy and Environment* 2019;6(3):7–15.
- [17] Ashraf H, Abdellatif SO, Elkholy MM, El-Fergany AA. Computational techniques based on artificial intelligence for extracting optimal parameters of PEMFCs: survey and insights. *Arch Comput Methods Eng* 2022;29(6):3943–72.
- [18] El-Fergany AA, Hasanien HM, Agwa AM. Semi-empirical PEM fuel cells model using whale optimization algorithm. *Energy Convers Manag* 2019;201:112197.
- [19] Ali ZM, Ahmed AM, Hasanien HM, Aleem SHA. Optimal design of fractional-order PID controllers for a nonlinear AWS wave energy converter using hybrid jellyfish search and particle swarm optimization. *Fractal and Fractional* 2023;8(1):6.
- [20] Ali ZM, Al-Dhaifallah M, Al-Gahtani SF, Muranaka T. A new maximum power point tracking method for PEM fuel cell power system based on ANFIS with modified manta ray foraging algorithm. *Control Eng Pract* 2023;134:105481.
- [21] Rizk-Allah RM, El-Fergany AA. Artificial ecosystem optimizer for parameters identification of proton exchange membrane fuel cells model. *Int J Hydrogen Energy* 2021;46(75):37612–27.
- [22] Gupta J, Nijhawan P, Ganguli S. Optimal parameter estimation of PEM fuel cell using slime mould algorithm. *Int J Energy Res* 2021;45(10):14732–44.
- [23] Priya K, Rajasekar N. Application of flower pollination algorithm for enhanced proton exchange membrane fuel cell modelling. *Int J Hydrogen Energy* 2019;44(33):18438–49.
- [24] Diab AAZ, Tolba MA, El-Magd AGA, Zaky MM, El-Rifaie AM. Fuel cell parameters estimation via marine predators and political optimizers. *IEEE Access* 2020;8:166998–7018.
- [25] Jiang B, Wang N, Wang L. Parameter identification for solid oxide fuel cells using cooperative barebone particle swarm optimization with hybrid learning. *Int J Hydrogen Energy* 2014;39(1):532–42.
- [26] Hao P, Sobhani B. Application of the improved chaotic grey wolf optimization algorithm as a novel and efficient method for parameter estimation of solid oxide fuel cells model. *Int J Hydrogen Energy* 2021;46(73):36454–65.
- [27] Guo C, Lu J, Tian Z, Guo W, Darvishan A. Optimization of critical parameters of PEM fuel cell using TLBO-DE based on Elman neural network. *Energy Convers Manag* 2019;183:149–58.
- [28] Li J, Gao X, Cui Y, Hu J, Xu G, Zhang Z. Accurate, efficient and reliable parameter extraction of PEM fuel cells using shuffled multi-simplex search algorithm. *Energy Convers Manag* 2020;206:112501.
- [29] Zhao W, Wang L, Mirjalili S. Artificial hummingbird algorithm: a new bio-inspired optimizer with its engineering applications. *Comput Methods Appl Mech Eng* 2022;388:114194.

- [30] Hamida MA, El-Sehiemy RA, Ginidi AR, Elattar E, Shaheen AM. Parameter identification and state of charge estimation of Li-Ion batteries used in electric vehicles using artificial hummingbird optimizer. *J Energy Storage* 2022;51:104535.
- [31] Sarhana S, Shaheen A, El-Sehiemy R, Gafar M. Optimal multi-dimension operation in power systems by an improved artificial hummingbird optimizer. *Hum.-Centric Comput. Inf. Sci* 2023;13:13.
- [32] El-Sehiemy R, Shaheen A, El-Fergany A, Ginidi A. Electrical parameters extraction of PV modules using artificial hummingbird optimizer. *Sci Rep* 2023;13(1):9240.
- [33] Moustafa G, Ginidi AR, Elshahed M, Shaheen AM. Economic environmental operation in bulk AC/DC hybrid interconnected systems via enhanced artificial hummingbird optimizer. *Elec Power Syst Res* 2023;222:109503.
- [34] Mann RF, Amphlett JC, Hooper MA, Jensen HM, Peppley BA, Roberge PR. Development and application of a generalised steady-state electrochemical model for a PEM fuel cell. *J Power Sources* 2000;86(1–2):173–80.
- [35] Mahato DP, Sandhu JK, Singh NP, Kaushal V. On scheduling transaction in grid computing using cuckoo search-ant colony optimization considering load. *Cluster Comput* 2020;23:1483–504.
- [36] Singla MK, Nijhawan P, Oberoi AS. Parameter estimation of three diode solar PV cell using chaotic dragonfly algorithm. *Soft Comput* 2022;26(21):11567–98.
- [37] Rani S, Babbar H, Kaur P, Alshehri MD, Shah SHA. An optimized approach of dynamic target nodes in wireless sensor network using bio inspired algorithms for maritime rescue. *IEEE Trans Intell Transport Syst* 2022.